Fast half-quadratic regularized phase tracking for non normalized fringe patterns

Ricardo Legarda-Saenz

Facultad de Matematicas. Universidad Autonoma de Yucatan
Apartado Postal 172. 97110 Merida, Yucatan. Mexico

rlegarda@tunku.uady.mx

Mariano Rivera

Centro de Investigaciones en Matematicas, A. C.
Apartado Postal 402. 36000 Guanajuato, Guanajuato. Mexico

mrivera@cimat.mx

Although one of the simplest and powerful approaches for the demodulation of a single fringe pattern with closed fringes is the regularized phase tracking (RPT) technique, this technique has two important drawbacks: its sensibility at the fringe-pattern modulation and the time employed in the estimation. In this paper we present modifications to the RPT technique which consist of the inclusion of a rough estimate of the fringe-pattern modulation, and the linearization of the fringe-pattern model which allow the minimization of the cost function through stable numerical linear techniques. With these changes, the demodulation of non-normalized fringe patterns is made with a significant reduction in the processing time, preserving the demodulation accuracy of the original RPT method.

OCIS codes: 100.2650, 100.5070, 120.5050, 120.3940

1. Introduction

The main goal of fringe analysis techniques is to recover accurately the local modulated phase from one or several fringe patterns;[1] such phase is related to some physical quantities like shape, deformation, refractive index, temperature, etc. The basic model for a fringe pattern is given by

$$I_r = a_r + b_r \cos\left(f_r\right) + \eta_r \tag{1}$$

where $r = (r_x, r_y)^T \in L$ denotes a pixel position in the lattice L, a_r is the background illumination, b_r is the amplitude modulation, η_r represents additive independent noise (generally assumed with a Gaussian distribution) and f_r is the phase map to be recovered.

There is a number of well-known techniques to estimate the phase term. In experiments with controlled conditions, the first choice is to use a phase shifting technique for the phase estimation.[1] However, in some experiments like the investigation of transient mechanical processes, it is difficult to acquire multiple fringe-patterns. In such situations, the phase estimation has to be done with a single fringe-pattern that contains, in general, closed and noisy fringes with large variations in the fringe modulation.

Several successful attempts can be found in the literature for the demodulation of a single fringe pattern with closed fringes,[2−3] where one of the simplest and powerful approaches is the regularized phase tracking (RPT) technique.[4−5] Despite their accurate phase-estimate, a disadvantage of the RPT technique is its sensitivity at the fringe-pattern modulation. This means that the fringe pattern has to be preprocessed to remove the background illumination and amplitude modulation.

To correct this problem, it was reported an improvement of the RPT technique,[5] which consists in the addition of one term that models the fringe pattern modulation. With this new term, the improved RPT technique can successfully estimate the phase of non-normalized fringe patterns that the original RPT formulation fails to recover. However, the minimization in this proposed cost function is still a nonlinear process which increases notably the time employed in the phase estimation.

In this paper, we present modifications to the RPT technique which consist of the inclusion of a rough estimate of the fringe-pattern modulation, and the linearization of the fringe-pattern model which allow the minimization of the cost function through linear techniques. These modifications produce a significant reduction in the processing time using a stable numerical minimization algorithm without any significant change in the demodulation accuracy, allowing the demodulation of non-normalized fringe patterns.

The organization of the paper is a follows: Section 2 briefly describes the basic RPT technique. Section 3 explains the proposed modifications to the RPT technique and presents an efficient numerical minimization algorithm. Section 4 shows the performance of the proposed modifications on examples of synthetic and experimental fringes patterns, and section 5 offers concluding remarks.

2. Brief review of the Regularized Phase Tracking technique

The RPT technique assumes that the fringe pattern may locally be considered monochromatic.[4−5] Consequently, it can be modelled as a cosinusoidal function (equation (1)) where the phase term is assumed to be smooth and can be approximated locally by a plane. The

basic cost function for the RPT technique is defined as[4]

$$U(p_r) = \sum_{s \in \mathcal{N}_r} \left\{ \left[I_s^h - \cos\left(p_r(s)\right) \right]^2 + \left[I_s^h - \cos\left(p_r(s) + \alpha\right) \right]^2 + \lambda \left[f_s - p_r(s) \right]^2 m_s \right\} \quad (2)$$

where the local phase, f, and the local frequencies, $\omega = (u, v)^T$, are estimated at the pixel r; the fringe pattern I_s^h is a high-pass filtered version of the fringe pattern given by equation (1), that is $I_s^h \approx \cos(f_s)$; $\mathcal{N}_r = \{s : s \in L, |r - s|_M \leq d\}$ is the neighborhood region around r with coordinates $s = (s_x, s_y)^T$ where $|z|_M = |z_1| + |z_2| + ...|z_n|$ is the Manhattan norm and d is an integer parameter that determines the size of the neighborhood; m_s is an indicator field that is equal to one if the phase f_s at the site s has already been estimated, and zero otherwise, α is a constant value used to constrain the phase estimate to a smooth solution, and λ is the regularizing parameter that controls (along with the size of $\mathcal{N}_r$) the smoothness of the detected phase.[4] The value of λ is selected interactively because there is not a precise method for the choice of the regularization values.[6] The function

$$p_r(s) = f_r + \omega_r^T (r - s) \quad (3)$$

is the planar model used for estimating the phase at the position s using the parameters at position r. The fundamental idea in the RPT technique is that given the phase and the local frequency at position r, the phase f_s can be fitted into a small neighborhood around pixel r with a plane assuming smooth phase field. To estimate the phase field with the RPT technique, it is needed to minimize the cost function given in equation (2) at each point r with respect to the local phase f and the local frequency ω. The estimated phase is continuous, and, consequently, no further unwrapping process has to be done. Several variants of the basic RPT technique can be found in the literature.[4−5]

3. Improvements in the Regularized Phase Tracking technique

3.A. Introducing a rough modulation estimate in the RPT technique

One drawback of the basic RPT technique is the need of the fringe-pattern normalization, that is, $I_s^h \approx \cos(f_s)$ must be satisfied. This means that any deviation from normalized fringes will generate errors in the phase estimation.[5,3,7] An option to solve this problem is to reduce the contributions of the terms a and b from equation (1) by means of a filtering process before the phase estimation.[7,8] The background term a can be removed without difficulty,[2] but the filtering process tends to fail especially in regions with noisy and low-contrast visibility because the modulation is removed by a division of small values of b at those sites.[5]

Recently, an alternative was reported in reference 5 which consist of the addition of one term that models the fringe pattern modulation. With this new term, the RPT technique can successfully estimate the phase of non-normalized fringe patterns by only removing the background term from the original fringe pattern. However, this modification increases notably the time employed in the estimation process, and the results obtained in regions with saddle points or very low frequencies are spurious.

A practical solution is to process the fringe pattern in such a way that a rough estimate of the modulation can be obtained.[3,7,8] Instead of removing the fringe-pattern modulation using a division, it is included in the cost function given in equation (2) as

$$U(p_r) = \sum_{s \in \mathcal{N}_r} \left\{ \left[g_s - \hat{b}_s \cos\left(p_r(s)\right) \right]^2 + \left[g_s - \hat{b}_s \cos\left(p_r(s) + \alpha\right) \right]^2 + \lambda \left[f_s - p_r(s) \right]^2 m_s \right\} \quad (4)$$

where $\hat{b}$ is the estimated modulation computed from a filtering process,[7,8] and the fringe pattern is assumed as

$$g_r \approx b_r \cos\left(f_r\right) \quad (5)$$

where the background illumination term a_r was removed using, for instance, a membrane filter.[2]

With this simple modification shown in equation (4), the RPT technique improves significantly the robustness of the phase estimation of fringe patterns with variations in the fringe-pattern modulation, as it can be seen in the experiments shown in section 4.

3.B. Proposed half-quadratic cost function for the RPT technique

However, the minimization of the cost function (4) leads to solve a non-linear problem using time consuming methods like the Broyden-Fletcher-Goldfarb-Shanno.[9,10] Moreover, this kind of methods does not guarantee uniqueness of the solution; as a consequence, a good initial value must always be provided to avoid to be trapped into local minimums of the function.[10] An alternative was published recently,[3] where it is proposed a half-quadratic cost function for the phase estimation, which consist of the linearization of the fringe-pattern model and the minimization of the resultant cost function through alternate solutions of linear systems; the robustness of the minimization process is improved by introducing a outlier detection and rejection strategy.

Following the ideas expressed in reference 3, it is assumed that the phase term can be expressed as

$$f = \hat{f} + \tilde{f} \quad (6)$$

where $\hat{f}$ is a known approximation of the phase f and $\tilde{f}$ is an unknown residual phase-value. If the approximation $\hat{f}$ is close enough to f, then first order Taylor series approximate very well the fringe model given in equation (5).[3] This can be expressed as

$$E(\tilde{f}_r; \hat{f}_r) = g_r - \hat{b}_r \left[\cos\left(\hat{f}_r\right) - \tilde{f}_r \sin\left(\hat{f}_r\right)\right] \approx 0. \tag{7}$$

As it can be observed, if a good approximation of both the phase value and modulation estimate at the pixel r exist, then it is only needed to estimate the residual term $\tilde{f}$, and such minimization is a linear process. The robustness of such estimation is improved by introducing an outlier detection and rejection strategy because it is common to have large residuals at noisy regions, and, therefore, the pixels with large residuals need to be treated as outliers.

For the particular case of the RPT cost function, the model phase given in equation (3) is approximated using the approach described previously. In the same way that the phase term was expressed in equation (6), the frequency is approximated as

$$\omega = \hat{\omega} + \tilde{\omega} \tag{8}$$

where $\hat{\omega}$ (as $\hat{f}$) is a known approximation of the frequency and $\tilde{\omega}$ is an unknown residual. Thus, by defining

$$\hat{p}_r(s) = \hat{f}_r + \hat{\omega}_r^T (r - s) \tag{9}$$

and

$$\tilde{p}_r(s) = \tilde{f}_r + \tilde{\omega}_r^T (r - s) \tag{10}$$

the model for the fringe pattern is rewritten as

$$\begin{aligned} \hat{b}_s \cos\left(p_r(s)\right) &= \hat{b}_s \cos\left(\hat{p}_r(s) + \tilde{p}_r(s)\right) \\ &\approx \hat{b}_s \left[\cos\left(\hat{p}_r(s)\right) - \tilde{p}_r(s) \sin\left(\hat{p}_r(s)\right)\right] \\ &= \hat{b}_s \left[\cos\left(\hat{f}_r + \hat{\omega}_r^T(r-s)\right) - \left(\tilde{f}_r + \tilde{\omega}_r^T(r-s)\right) \sin\left(\hat{f}_r + \hat{\omega}_r^T(r-s)\right)\right] \end{aligned} \tag{11}$$

As it can be seen in the previous equation, if an estimation of the modulation is available, and a good approximation of the phase and the frequency at the pixel r exits, it is only needed to estimate the residual terms. In the same way that equation (7), the estimation of such terms becomes a linear process; that is

$$E(\tilde{f}_r, \tilde{\omega}_r; \hat{f}_r, \hat{\omega}_r) = g_r - \hat{b}_r \left[\cos\left(\hat{p}_r(s)\right) - \tilde{p}_r(s) \sin\left(\hat{p}_r(s)\right)\right] \approx 0. \tag{12}$$

We introduced the approximation shown in equation (12) and the estimated modulation, $\hat{b}$, in the RPT cost function. The proposed cost function for the RPT technique consists of computing the residual terms $\tilde{f}_r$ and $\tilde{\omega}_r$, and the outlier detector l_s. They are the minimizers of the following regularized half-quadratic cost function

$$U(\tilde{f}_r, \tilde{\omega}_r, l_s) = \frac{1}{2} \sum_{s \in \mathcal{N}_r} \left\{ \begin{array}{ll} & l_s^2 \left[g_s - \hat{b}_s \cos\left(\hat{p}_r(s)\right) + \tilde{p}_r(s) \hat{b}_s \sin\left(\hat{p}_r(s)\right) \right]^2 \\ + & l_s^2 \left[g_s - \hat{b}_s \cos\left(\hat{p}_r(s) + \alpha\right) + \tilde{p}_r(s) \hat{b}_s \sin\left(\hat{p}_r(s) + \alpha\right) \right]^2 \\ + & \lambda \left[f_s - \hat{p}_r(s) - \tilde{p}_r(s) \right]^2 \quad l_s^2 + \mu \left(1 - l_s\right)^2 \end{array} \right\} \tag{13}$$

where $l_s \in [0, 1]$ act as an indicator variable that weighs the individual contribution of the data, and μ is a positive parameter that control the outliers detection. The values of μ and λ are selected interactively because there is not a precise method for the choice of the regularization values.[6] The rest of the terms are equivalent to the definitions given in equations (2) and (4).

3.C. Minimization of the proposed cost function

The proposed RPT cost function shown in equation (13) is half-quadratic in the sense that it is quadratic with respect to the residual terms $\tilde{f}_r$ and $\tilde{\omega}_r$ when the outlier detector l_s is fixed, and it is convex with respect to l_s when $\tilde{f}_r$ and $\tilde{\omega}_r$ are fixed.[11−12] So, given initial values for $\hat{f}$ and $\hat{\omega}$, the residuals terms and the outlier term are estimated in two steps. In the first step, the outlier term l_s is estimated using the following equation, resultant of equating the partial gradient of (13) with respect to l_s,

$$l_s = \frac{\mu}{\mu + E_0^2 \left[p_r(s) \right] + E_1^2 \left[p_r(s) \right]} \tag{14}$$

where $E_0 \left[. \right]$ and $E_1 \left[. \right]$ are defined in equation (A5) in Appendix A. Note that $l_s \approx 1$ for those sites where the difference between the input data and the estimate are small with respect to μ, and $l_s \approx 0$ for those pixels where the model does not fit the model very well, so the regularization term μ has more control over the computation of the residual terms $\tilde{f}_r$ and $\tilde{\omega}_r$.

Once the outlier term was estimated, the linear system that results of equating the partial gradient of (13) with respect to the residual terms $\tilde{f}_r$ and $\tilde{\omega}_r$ is solved. The second step consist of updating the values $\hat{f}$ and $\hat{\omega}$ by the estimated residual terms, that is $\hat{f}_r = \hat{f}_r + \tilde{f}_r$ and $\hat{\omega}_r = \hat{\omega}_r + \tilde{\omega}_r$.

These two steps are iterated until convergence which is guaranteed if the computed residual terms $\tilde{f}_r$ and $\tilde{\omega}_r$ are small so that

$$\begin{aligned}\left\|g_r - \hat{b}_r \cos\left(\hat{p}_r(s)\right)\right\| &\geq \left\|g_r - \hat{b}_r \left[\cos\left(\hat{p}_r(s)\right) - \tilde{p}_r(s)\sin\left(\hat{p}_r(s)\right)\right]\right\| \\ &\approx \left\|g_r - \hat{b}_r \cos\left(\hat{p}_r(s) + \tilde{p}_r(s)\right)\right\|\end{aligned}$$

For our minimization problem, each step of the minimization process is achieved by a Gauss-Seidel scheme.[13] Given that the cost function (13) is half-quadratic, the Gauss-Seidel scheme converges to the global minimum of the subproblems corresponding to each step previously mentioned. Therefore, each iteration reduces the cost function value, and the convergence to a local minimum, at least, is guaranteed because the cost function (13) is bounded by zero.[3,10,13]

The practical details of the minimization of the half-quadratic cost function (13) are given in the Algorithm 1, where we define

$$A_{rs} \stackrel{def}{=} l_s^2 \hat{b}_s^2 \left[\sin^2\left(\hat{p}_r(s)\right) + \sin^2\left(\hat{p}_r(s) + \alpha\right)\right] + \lambda m_s \tag{15}$$

and

$$\begin{aligned}B_{rs} \stackrel{def}{=}\ & l_s^2 \left[g_s - \hat{b}_s \cos\left(\hat{p}_r(s)\right)\right] \hat{b}_s \sin\left(\hat{p}_r(s)\right) \\ +\ & l_s^2 \left[g_s - \hat{b}_s \cos\left(\hat{p}_r(s) + \alpha\right)\right] \hat{b}_s \sin\left(\hat{p}_r(s) + \alpha\right) \\ -\ & \lambda m_s \left[f_s - \hat{p}_r(s)\right]\end{aligned} \tag{16}$$

Algorithm 1 shows the Gauss-Seidel scheme for the minimization of the proposed RPT technique. The derivation of the Gauss-Seidel formulas are shown in Appendix A; note that such formulas are simplified to those in Algorithm 1 if the coarse parameters, $\hat{f}_r$ and $\hat{\omega}_r$, are updated after each residual is computed.

Step 6 in Algorithm 1 can be implemented by different ways, the most successful one consist of constraining the search to a single fringe choosing at each iteration the pixel r with the largest fringe pattern irradiance.[14–5,15]

4. Experimental Results and Discussion

To illustrate the performance of the proposed RPT cost function, some experiments were made in a 1.5-GHz-Intel-Pentium-M PC with one GB of main memory. In these experiments the performances of the improved RPT method reported in reference 5, the RPT cost function defined in equation (4), and the proposed cost function defined in equation (13) are compared. In each experiment, the parameters values and the seed position were the same for all methods, and the fringe modulation of the experimental fringes were estimated using Fourier filtering.[7]

In the first experiment, we compared the performances of the above RPT techniques in the demodulation of a synthetic fringe-pattern with 256 x 256 pixels shown in figure 1, panel (a).

Panels (b) and (c) show the synthetic modulation and phase, respectively, used to generate the fringe pattern. The synthetic modulation shown in panel (b) was used as the term $\hat{b}$ in equations (4) and (13). The resultant demodulations are shown in figure 2. The time employed and the estimation errors are shown in table 1 where the parameters were $\lambda = 1$, $\alpha = 0.1\pi$, and the neighborhood region was a 9 x 9 window ($d = 4$) for the cost functions given in equations (4) and (13). In the case of the RPT method reported in reference 5, the neighborhood region was a 11 x 11 window ($d = 5$) because it is necessary to increase the window size to track the frequencies of the fringe-pattern modulation.[5]

From the results shown in figure 2 and table 1, we can stress some points: the original RPT technique shown in equation (2) always fails to recover the phase term from a non-normalized fringe pattern, even in the case of very smooth modulation like the shown in figure 1, panel (b). This situation was solved partially by the method reported in reference 5 because it can accurately estimate the phase in most of the fringe pattern, except at the center of the fringe-pattern given that the method can not detect the low frequency of this region.

An accurate phase-estimate is obtained when an estimation of the modulation in the RPT cost function is included, equation (4). In this case, the computation of the phase is successfully made with accuracy as it can be seen in the results reported in table 1 and figure 2. Most of the errors can be founded at the center fringe-pattern due to the neighborhood region is not large enough to detect the low frequency. Additionally, the time employed in the phase estimation is significatively reduced using the proposed cost function defined in equation (13), without any major change in the demodulation accuracy.

A second experiment was made with the fringe pattern shown in figure 3, panel (a). This synthetic fringe pattern was generated using the phase term shown in figure 1, panel (c) and the synthetic modulation shown in figure 3, panel (b). The resultant demodulations and the time employed are shown in figure 3 and table 2, respectively. The same parameter of the first experiment was used here. As it can be seen in the resultant estimates, the great performance of the proposed cost function is maintained even in situations with large variations of the modulation as it can be seen in the modulation shown in figure 3, panel (b).

The third experiment shows the importance of the modulation estimate in the performance of the proposed cost function. We generated some synthetic fringe-patterns with different levels of modulation using the phase field shown in figure 1, panel (c). For every fringe pattern, we estimated roughly the modulation using a Fourier filtering[7] and this estimate was included as the term $\hat{b}$ in the equation (13). The fringe patterns and the estimate of the modulation are shown in figure 4, panels (a) to (f), and the resultant phase-estimate are shown in panels (g) to (i). In the case of the first column of the Figure 4, an accurate phase-estimate was obtained using a low fringe-pattern modulation, with the exception of

the errors due to low frequencies, as it was previously explained. This is due to the good estimation of the modulation, as it can be seen in the panel (d) of Figure 4. The erroneous phase-estimate due to the modulation are in the second and third columns of the Figure 4, where it is evident that the errors are located only in regions with a very low or nearly to zero fringe-pattern modulation, as it can be seen in the panels (e) and (f) of Figure 4. As it may be observed, an accurate phase-estimate will be obtained with the proposed cost function defined in equation (13) only if the fringe pattern has levels of modulation that can be detected by the modulation-estimation technique.

The advantage of the fast estimation without significant change in accuracy is evident in the processing of experimental fringe patterns with large size. The last experiment was the demodulation of an experimental fringe pattern shown in figure 5, panel (a). An estimate of the modulation was obtained by Fourier filtering[7] and used as the term $\hat{b}$ in equations (4) and (13). The resultant demodulations are shown in panels (b) to (d) and the time employed is shown in table 3. The parameters used for this experiment were $\lambda = 0.5$, $\alpha = 0.1\pi$, and the neighborhood region was a 13 x 13 window ($d = 6$) for the cost functions given in equations (4) and (13). In the case of the RPT method reported in reference 5, it was a 15 x 15 window ($d = 7$). As it can be seen in the results of this experiment, the difference in time are evident when it is necessary to process large images or to increase the size of the neighborhood region $\mathcal{N}_r$ to detect the slope terms of the plane model.[5]

5. Conclusions

In this paper we present a modified RPT technique for the fast demodulation of non normalized fringe patterns which consist of the inclusion of a rough estimate of the fringe-pattern modulation, and the linearization of the fringe-pattern model that allow the minimization of the cost function through linear techniques.

The changes allow the demodulation of non-normalized fringe-patterns with a significant reduction in the processing time, preserving the demodulation accuracy of the original RPT method. These are shown on examples of demodulation of synthetic and experimental fringe-patterns. Additionally, we include the details of the minimization algorithm in the Algorithm 1 and the Appendix A.

Appendix A. Gauss-Seidel Updating Formulas

From the chain rule we have that

$$\frac{\partial U\left(\tilde{p}_r(s)\right)}{\partial \tilde{f}_r} = \frac{\partial U\left(\tilde{p}_r(s)\right)}{\partial \tilde{p}_r(s)} \frac{\partial \tilde{p}_r(s)}{\partial \tilde{f}_r}$$

and

$$\frac{\partial U\left(\tilde{p}_r(s)\right)}{\partial \tilde{\omega}_r} = \frac{\partial U\left(\tilde{p}_r(s)\right)}{\partial \tilde{p}_r(s)} \frac{\partial \tilde{p}_r(s)}{\partial \tilde{\omega}_r}.$$

Therefore

$$\frac{\partial U\left(\tilde{p}_r(s)\right)}{\partial \tilde{p}_r(s)} = \sum_{s \in \mathcal{N}_r} \left[\tilde{f}_r + \tilde{\omega}_r^T (r-s)\right] A_{rs} + B_{rs};$$

where A_{rs} and B_{rs} are defined in equations (15) and (16), respectively.

Now, given that $\frac{\partial \tilde{p}_r(s)}{\partial \tilde{f}_r} = 1$, we have the Gauss-Seidel iteration formula by equaling to zero the partial derivative and solving for $\tilde{f}_r$

$$\tilde{f}_r = \frac{-\sum_{s \in \mathcal{N}_r} \left[\tilde{\omega}_r^T (r-s) A_{rs} + B_{rs}\right]}{\sum_{s \in \mathcal{N}_r} A_{rs}}. \tag{A1}$$

On the other hand:

$$\nabla_{w_r} \tilde{p}_r(s) = \left[\frac{\partial \tilde{p}_r(s)}{\partial \tilde{u}_r}, \frac{\partial \tilde{p}_r(s)}{\partial \tilde{v}_r}\right]^T = \left[r_x - s_x, r_y - s_y\right]^T.$$

Therefore, the Gauss-Seidel iteration formulas for updating the local frequency are:

$$\tilde{u}_r = \frac{-\sum_{s \in \mathcal{N}_r} \left[\left(\tilde{f}_r + \tilde{v}_r (r_y - s_y)\right) A_{rs} + B_{rs}\right] (r_x - s_x)}{\sum_{s \in \mathcal{N}_r} A_{rs} \left(r_x - s_x\right)^2}. \tag{A2}$$

and

$$\tilde{v}_r = \frac{-\sum_{s \in \mathcal{N}_r} \left[\left(\tilde{f}_r + \tilde{u}_r (r_x - s_x)\right) A_{rs} + B_{rs}\right] (r_y - s_y)}{\sum_{s \in \mathcal{N}_r} A_{rs} \left(r_y - s_y\right)^2}. \tag{A3}$$

Finally, the outlier rejection field iteration formula is obtained from $\frac{\partial U(\tilde{p}_r(s))}{\partial \tilde{l}_s} = 0$:

$$l_s = \frac{\mu}{\mu + E_0^2\left[p_r(s)\right] + E_1^2\left[p_r(s)\right]} \tag{A4}$$

where

$$\begin{aligned} E_0\left[p_r(s)\right] &\stackrel{def}{=} g_s - \hat{b}_s \cos\left(\hat{p}_r(s)\right) + \tilde{p}_r(s) \hat{b}_s \sin\left(\hat{p}_r(s)\right) \\ E_1\left[p_r(s)\right] &\stackrel{def}{=} g_s - \hat{b}_s \cos\left(\hat{p}_r(s) + \alpha\right) + \tilde{p}_r(s) \hat{b}_s \sin\left(\hat{p}_r(s) + \alpha\right) \end{aligned} \tag{A5}$$

Acknowledgments

The authors thank to Luis A. Rodriguez for his helpful proof-reading. R. Legarda-Saenz was supported in part by grants from the Programa de Impulso y Orientacion a la Investigacion (Universidad Autonoma de Yucatan) and the Programa de Mejoramiento del Profesorado (SEP, Mexico). M. Rivera was supported in part by CONACYT (Mexico) under grants 40722 and 46270.

References

1. D. W. Robinson and G. T. Reid, eds., *Interferogram Analysis: Digital Fringe Pattern Measurement Techniques* (Institute of Physics, Bristol, 1993).
2. J. L. Marroquin, M. Rivera, S. Botello, R. Rodriguez-Vera, and M. Servin, "Regularization methods for processing fringe-pattern images," Appl. Opt. **38**, 788 – 794 (1999).
3. M. Rivera, "Robust phase demodulation of interferograms with open or closed fringes," J. Opt. Soc. Am. A **22**, 1170 – 1175 (2005).
4. M. Servin, J. L. Marroquin, and F. J. Cuevas, "Demodulation of a single interferogram by use of a two-dimensional regularized phase-tracking technique," Appl. Opt. **36**, 4540 – 4548 (1997).
5. R. Legarda-Saenz, W. Osten, and W. Juptner, "Improvement of the regularized phase tracking technique for the processing of non-normalized fringe patterns," Appl. Opt. **41**, 5519 – 5526 (2002).
6. M. Bertero and P. Boccacci, *Introduction to Inverse Problems in Imaging* (Institute of Physics Publishing, Bristol, 1998).
7. J. A. Quiroga and M. Servin, "Isotropic n-dimensional fringe pattern normalization," Opt. Commun. **224**, 221 – 227 (2003).
8. T. Kreis, *Holographic Interferometry. Principles and Methods* (Akademie Verlag, Berlin, 1996).
9. W. H. Press, S. A. Teukolsky, W. T. Vetterling, and B. P. Flannery, *Numerical Recipes in C*, 2nd ed. (Cambridge University Press, Cambridge, 1999).
10. J. Nocedal and S. J. Wright, *Numerical Optimization* (Springer Verlag, New York, 1999).
11. D. Geman and G. Reynolds, "Constrained restoration and the recovery of discontinuities," IEEE Transactions on Pattern Analysis and Machine Intelligence **14**, 367 – 383 (1997).
12. P. Charbonnier, L. Blanc-Feraud, G. Aubert, and M. Barlaud, "Deterministic edge-preserving regularization in computer imaging," IEEE Transactions on Image Processing **6**, 298 – 311 (1997).
13. G. H. Golub and C. F. Van Loan, *Matrix Computations* (Johns Hopkins U. Press, Baltimore, 1996).
14. J. Villa, J. A. Quiroga, and M. Servin, "Improved regularized phase tracking technique for the processing of squared-grating deflectograms," Appl. Opt. **39**, 502 – 508 (2000).
15. B. Strobel, "Processing of interferometric phase maps as complex-valued phasor images," Appl. Opt. **35**, 2192 – 2198 (1996).

Table 1. Time employed to demodulate the fringe pattern shown in figure 1

Method	Time employed (seconds)	RMS error(rad)
Equation (2)	54.2	3.76
Equation (4)	60.3	0.87
Equation (13)	13.6	0.89
Method from reference 5	135.7	1.12

The root mean square (RMS) error is computed by the difference between the estimated phase and the phase used to generate the fringe pattern

Table 2. Time employed to demodulate the fringe pattern shown in figure 3

Method	Time employed (seconds)	RMS error(rad)
Equation (4)	57.27	0.86
Equation (13)	16.94	0.97
Method from reference 5	129.98	1.13

The root mean square (RMS) error is computed by the difference between the estimated phase and the phase used to generate the fringe pattern

Table 3. Time employed to demodulate the fringe pattern shown in figure 5

Method	Time employed (seconds)
Equation (4)	205.2
Equation (13)	103.1
Method from reference 5	516.5

Algorithm 1 Gauss-Seidel Minimization Scheme

Set the initial parameters λ, μ;

Set $\tilde{f}_r = 0, \tilde{\omega}_r = 0, m_r = 0$, for all $r \in \mathcal{L}$;

Using equation (4), compute an initial phase f and an initial frequency ω at pixel r^0 and set $\mathcal{M} \leftarrow \{r^0\}$ and $m_{r^0} = 1$;

Give the tolerance $\epsilon > 0$;

while $\mathcal{M} \neq \mathcal{L}$ **do**

  Choose a pixel $r \in \mathcal{L} \backslash \mathcal{M}$ such that $\mathcal{N}_r \bigcap \mathcal{M} \neq \emptyset$;

  repeat

    Update the outlier rejection variable

$$l_s = \frac{\mu}{\mu + \left[g_s - \hat{b}_s \cos \hat{p}_r(s)\right]^2 + \left[g_s - \hat{b}_s \cos(\hat{p}_r(s) + \alpha)\right]^2} \quad \text{for all } s \in \mathcal{N}_r;$$

    Compute A_{rs} and B_{rs} with (15) and (16), respectively;

    Set $f_o = \hat{f}_r$;

    Compute the residual phase with

$$\tilde{f}_r = \frac{-\sum_{s \in \mathcal{N}_r} B_{rs}}{\sum_{s \in \mathcal{N}_r} A_{rs}};$$

    Set $\hat{f}_r = \hat{f}_r + \tilde{f}_r$ and then $\tilde{f}_r = 0$;

    Compute the residual horizontal frequency with

$$\tilde{u}_r = \frac{-\sum_{s \in \mathcal{N}_r} B_{rs}(r_x - s_x)}{\sum_{s \in \mathcal{N}_r} A_{rs}(r_x - s_x)^2};$$

    Set $\hat{u}_r = \hat{u}_r + \tilde{u}_r$ and then $\tilde{u}_r = 0$;

    Compute the residual vertical frequency with

$$\tilde{v}_r = \frac{-\sum_{s \in \mathcal{N}_r} B_{rs}(r_y - s_y)}{\sum_{s \in \mathcal{N}_r} A_{rs}(r_y - s_y)^2};$$

    Set $\hat{v}_r = \hat{v}_r + \tilde{v}_r$ and then $\tilde{v}_r = 0$;

  until $|\hat{f}_r - f_o| < \epsilon$;

  Set $m_r = 1$ and $\mathcal{M} = \mathcal{M} \bigcup \{r\}$;

end while

List of Figure Captions

List of Figures

1 (a) Synthetic fringe pattern. (b) Modulation, and (c) phase fields used to generate the fringe pattern. The phase field is wrapped for purpose of illustration. 18

2 Resultant phase estimate using: (a) equation (2), (b) method from reference 5, (c) equation (4), and (d) equation (13). Phase estimates are wrapped for the purpose of illustration. 19

3 (a) Synthetic fringe pattern. (b) Modulation field used to generate the fringe pattern. Resultant phase estimates using: (c) method from reference 5, (d) equation (4), and (e) equation (13). The phase field is wrapped for purpose of illustration. 20

4 (a)-(c) Synthetic fringe patterns with different levels of modulation. (d)-(f) Estimated modulation from fringe patterns shown in panels (a)-(c), respectively. (g)-(i) Resultant phase estimates using fringe pattern from panel (a)-(c) and the modulation from panels (d)-(f), respectively. The phase field is wrapped for purpose of illustration. 21

5 (a) Experimental fringe pattern. Resultant phase estimate using: (b) method from reference 5, (c) equation (4), and (d) equation (13). Phase estimates are wrapped for the purpose of illustration. 22

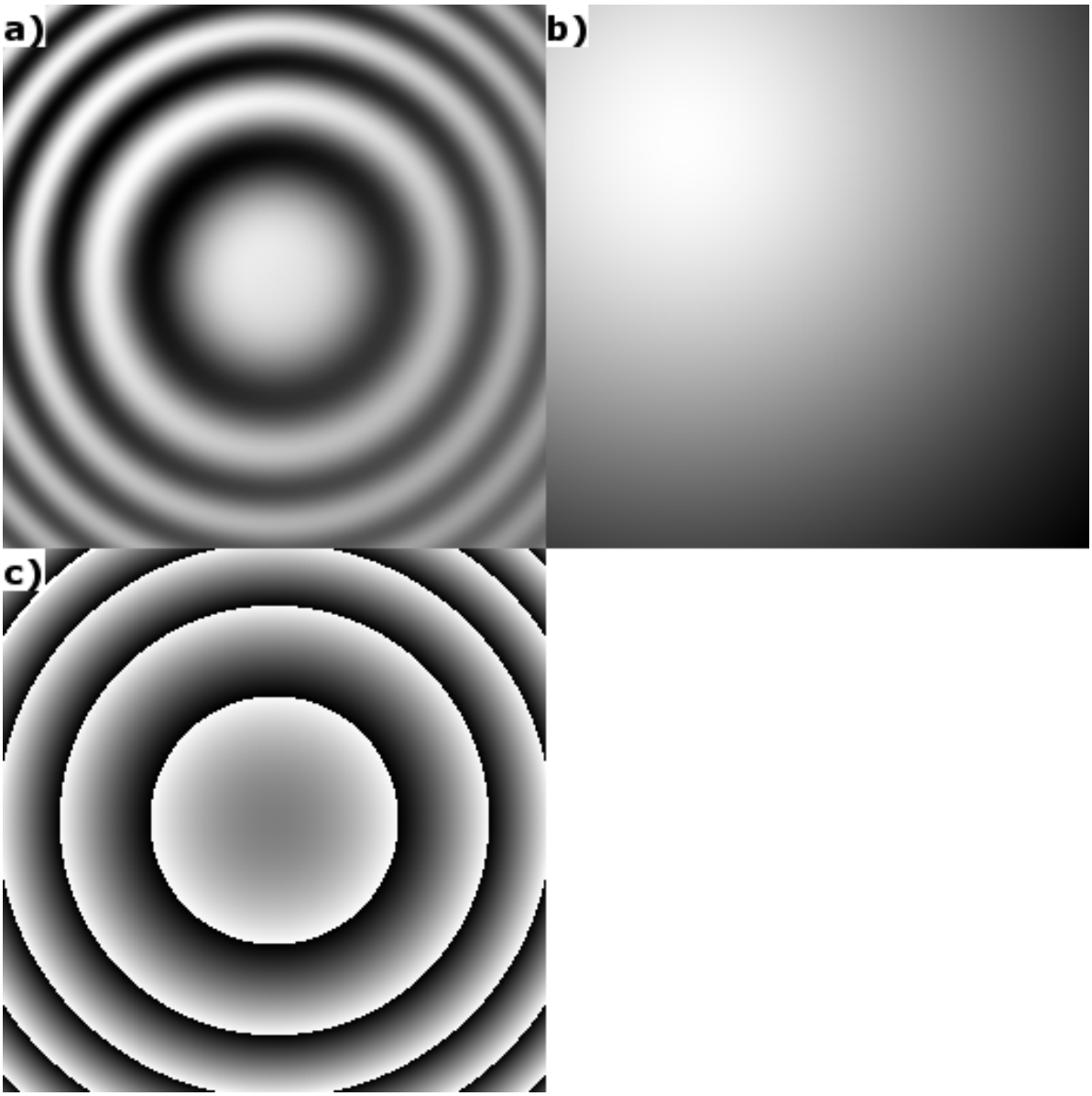

Fig. 1. (a) Synthetic fringe pattern. (b) Modulation, and (c) phase fields used to generate the fringe pattern. The phase field is wrapped for purpose of illustration.

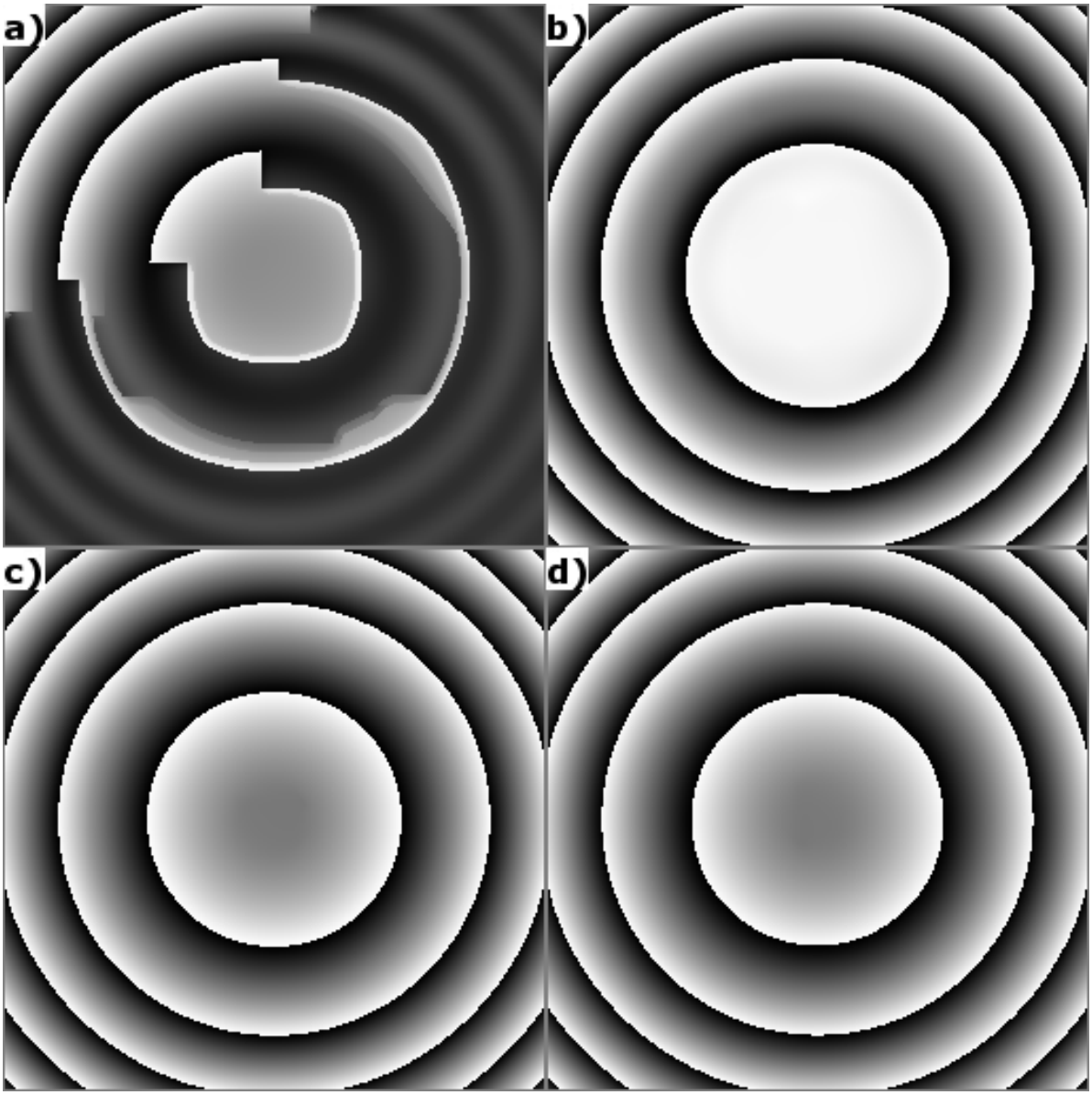

Fig. 2. Resultant phase estimate using: (a) equation (2), (b) method from reference 5, (c) equation (4), and (d) equation (13). Phase estimates are wrapped for the purpose of illustration.

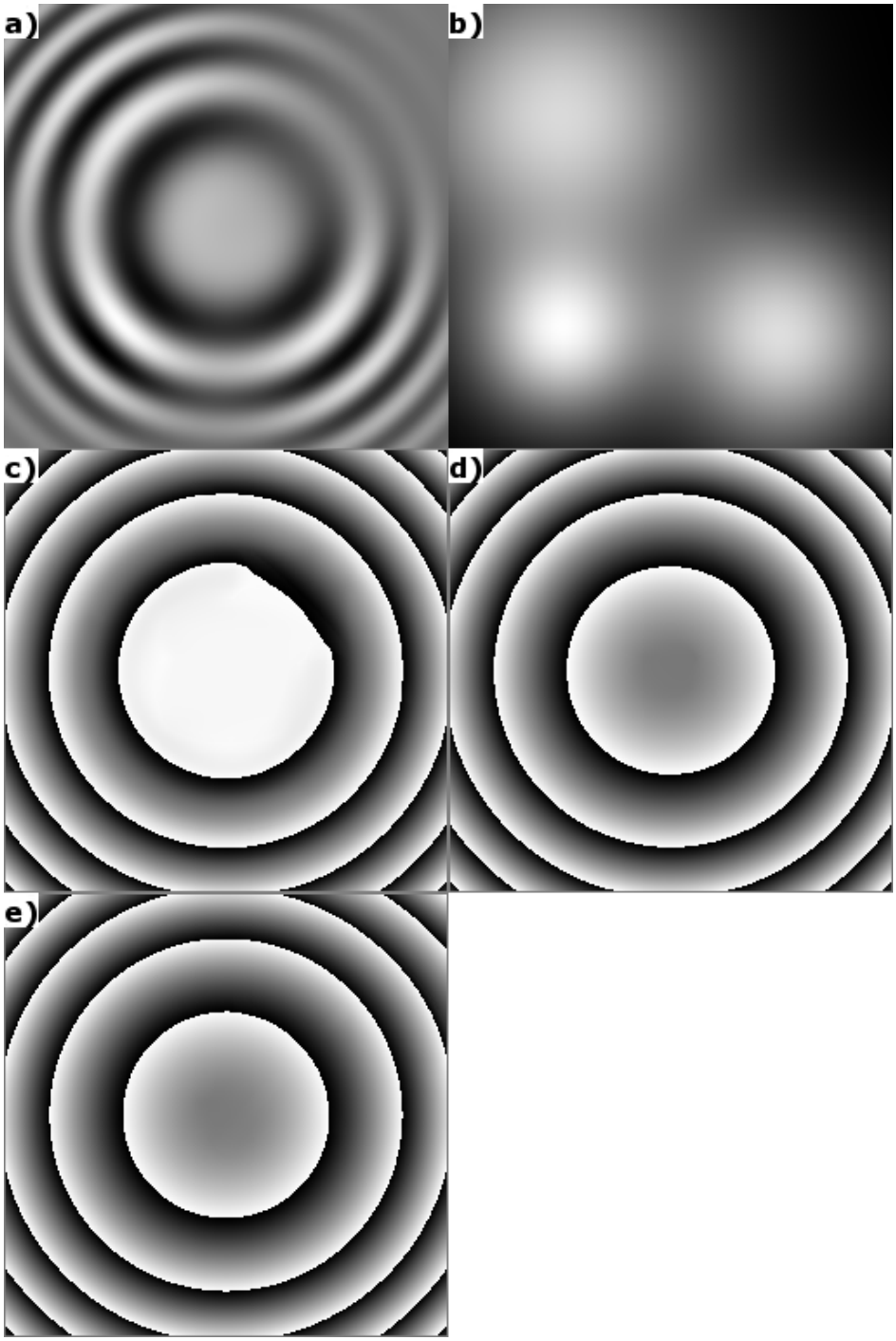

Fig. 3. (a) Synthetic fringe pattern. (b) Modulation field used to generate the fringe pattern. Resultant phase estimates using: (c) method from reference 5, (d) equation (4), and (e) equation (13). The phase field is wrapped for purpose of illustration.

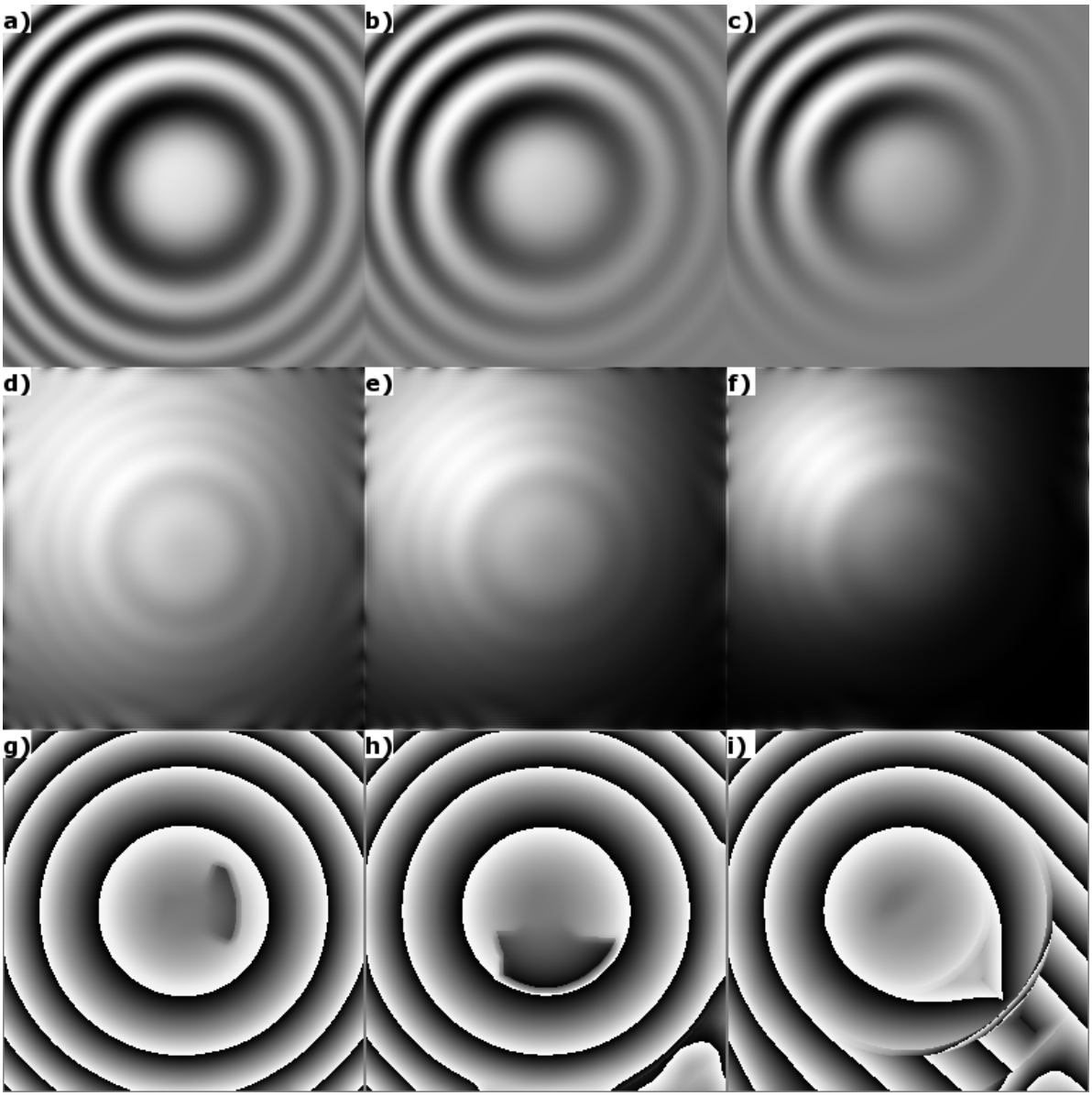

Fig. 4. (a)-(c) Synthetic fringe patterns with different levels of modulation. (d)-(f) Estimated modulation from fringe patterns shown in panels (a)-(c), respectively. (g)-(i) Resultant phase estimates using fringe pattern from panel (a)-(c) and the modulation from panels (d)-(f), respectively. The phase field is wrapped for purpose of illustration.

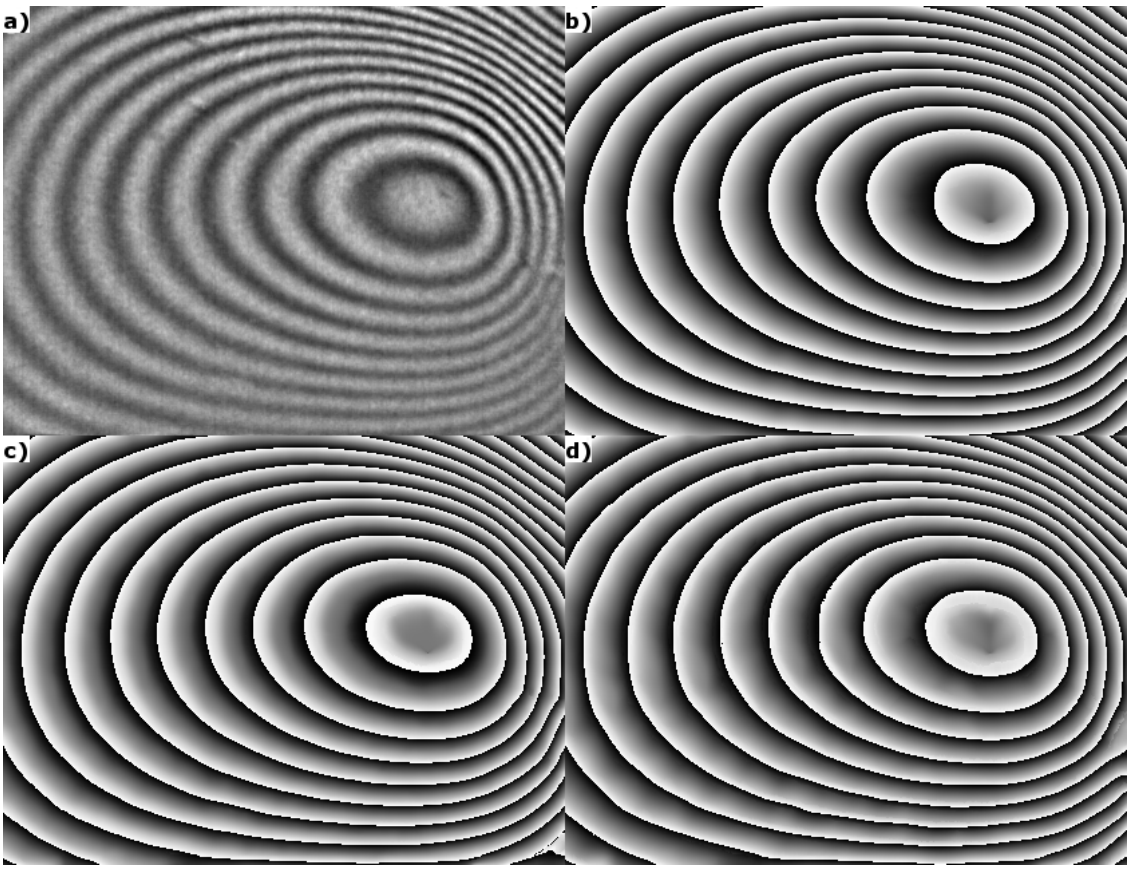

Fig. 5. (a) Experimental fringe pattern. Resultant phase estimate using: (b) method from reference 5, (c) equation (4), and (d) equation (13). Phase estimates are wrapped for the purpose of illustration.